Tellus
SERIES B
CHEMICAL
AND PHYSICAL
METEOROLOGY
PUBLISHED BY THE INTERNATIONAL METEOROLOGICAL INSTITUTE IN STOCKHOLM

Tellus (2009), 61B, 416–423
Printed in Singapore. All rights reserved

TELLUS

Investigation of parameters controlling the soil sink of atmospheric molecular hydrogen

By S. SCHMITT, A. HANSELMANN, U. WOLLSCHLÄGER, S. HAMMER and I. LEVIN*,
Institut für Umweltphysik, INF 229, 69120 Heidelberg, Germany

(Manuscript received 17 June 2008, in final form 24 October 2008)

ABSTRACT

Enclosure measurements have been performed on a bare mineral soil at an experimental field site near Heidelberg, Germany. From observed molecular hydrogen (H_2) mixing ratio changes in the enclosure, deposition velocities were calculated ranging from 8.4×10^{-3} to 8.2×10^{-2} cm s^{-1} and with an annual mean value of 3.1×10^{-2} cm s^{-1}. In the studied range of 2– 27 °C, the uptake showed a significant temperature dependence. However, this turned out not to be the primary driving mechanism of the uptake flux. Soil moisture content, co-varying with temperature, was identified as the major parameter being responsible for the diffusive permeability of H_2 in the soil and the final rate of H_2 uptake. A simple Millington–Quirk diffusion model approach could largely explain this behaviour and yielded a diffusion path length of H_2 in the studied soil of only 0.2–1.8 cm, suggesting that total H_2 consumption occurs within the first few centimetres of the soil. The diffusion model, when applied to continuous measurements of soil moisture content, atmospheric pressure, temperature and the mixing ratio of H_2 in the atmosphere, could largely reproduce the measured deposition flux densities, assuming a mean thickness of the diffusion path length of 0.7 cm.

1. Introduction

As a consequence of an expanding use of fuel cell technology, the mixing ratio of molecular hydrogen (H_2) in the troposphere may rise significantly due to leakages during H_2 production, storage and transport (Schultz et al., 2003; Tromp et al., 2003). As H_2 is oxidized in the troposphere by OH radicals, it acts as an indirect greenhouse gas consuming tropospheric OH, which would otherwise be available for the oxidation of CH_4 and other reduced trace gases. Furthermore, an increasing abundance of H_2 in the troposphere can result in elevated stratospheric H_2 and, after oxidation, in elevated water vapour in the stratosphere with a potentially large impact on the Earth's radiation balance and atmospheric chemistry (Tromp et al., 2003).

The present knowledge of the atmospheric H_2 budget is still rather qualitative because of the large uncertainties in its major sources and sinks (Novelli et al., 1999; Hauglustaine and Ehhalt, 2002). Especially the strength of the global soil sink, which is one of the dominating terms in the budget, is highly uncertain (e.g. Rhee et al., 2006). Estimates of this sink are generally obtained by scaling up local measurements of the H_2 deposition velocity v_d, assuming uniform atmospheric mixing ratios and a total effective deposition area. This, however, can be associated with large errors as the processes that control H_2 soil uptake are not well understood yet (Conrad, 1996 and references therein). Here, we present field measurements of H_2 soil uptake and its dependence on soil properties. A simple diffusion model describing flux kinetics is introduced, which may help to develop a better parametrization and upscaling of the regional and global loss rate of H_2.

*Corresponding author.
e-mail: ingeborg.levin@iup.uni-heidelberg.de
DOI: 10.1111/j.1600-0889.2008.00402.x

2. Basic considerations

Conrad and Seiler (1981) were the first to assume the destruction of H_2 in soils to be catalysed by different types of abiotic soil enzyme *hydrogenase*, following the reaction

$$H_2 \longleftrightarrow 2\,H^+ + 2\,e^-. \quad (1)$$

This enzymatic reaction is probably the basic process responsible for the uptake of atmospheric H_2 (Guo and Conrad, 2008). However, atmospheric H_2 has no unlimited access to the catalytic centre of the enzymes since the surrounding soil acts as a diffusion barrier (Conrad, 1996; Yonemura et al., 2000a). Hence, the limiting effect of diffusion must also be taken into account when estimating H_2 uptake rates. The temporal H_2 mixing ratio change dC_e/dt inside an enclosure setup (as in our experiment, see Fig. 1), therefore, has to be described with respect to the two basic processes: enzymatic destruction and gas diffusion.

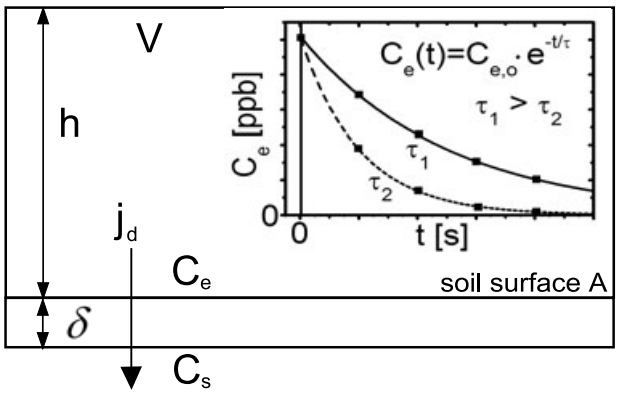

Fig. 1. Scheme of the enclosure setup. The inlay shows the temporal evolution of the H_2 mixing ratio inside the enclosure for two different uptake rates, respectively, decay times τ. C_e and C_s are the H_2 mixing ratios in the enclosure, respectively, in the soil, δ is the thickness of the flux restricting layer, V (=67.5 L) and h (=27 cm) are volume and height of the enclosure and j_d is the diffusive flux density of H_2 into the soil.

We assume an enclosure of volume V and height h being deployed to the investigated soil area A (Fig. 1). We further assume homogeneous distribution of C_e in V, while C_s is the H_2 mixing ratio in the soil air nearby the catalytic centre of the enzymes below a flux restricting layer of thickness δ. C_s and C_e are considered dimensionless molar mixing ratios throughout the whole text. If H_2 from a reservoir of volume V with mixing ratio C_e has to pass through a restricting layer of surface A and thickness δ to reach the catalytic centre of the enzyme, the temporally changing volume flux of H_2 through this layer, according to Fick's first law, is given by

$$jA = -P_{H_2}\frac{C_e - C_s}{\delta}A, \tag{2}$$

jA is the H_2 volume flux in ($m^3\,s^{-1}$), $C_e - C_s$ is the mixing ratio difference of H_2 over the restricting layer and P_{H_2} the molecular diffusive permeability of H_2 in the soil air. We assume a temporally changing linear gradient $(C_e - C_s)/\delta$ over the uppermost inactive soil layer of height δ. This assumption is necessary for our simple approach and follows the model assumptions by Yonemura et al. (2000a). Yonemura et al. (2000a) justify this assumption by their experimental findings of a significantly lowered uptake rate for H_2 in the first few centimetres of the soil. The volume flux in (2) equals the temporal change of H_2 in V that is given by $V(dC_e/dt)$, that is,

$$\frac{dC_e}{dt} = -P_{H_2}\frac{C_e - C_s}{\delta}\frac{A}{V}, \tag{3}$$

where dC_e/dt is the temporal mixing ratio change in the volume caused by diffusive flux. The substrate (here: hydrogen) destruction of an enzyme is given by the Michaelis–Menten equation, a well-established relation which describes the dependence of the substrate destruction rate dC_s/dt of an enzyme on the substrate mixing ratio C_s at the catalytic centre. For low H_2 mixing ratios in the soil air ('low mixing ratios' means mixing ratios for which in the derivation of the Michaelis–Menten equation the expression of the form $-(AC_s)/(B + C_s)$ can be replaced by $-C_s$. This replacement is justified if the mixing ratio of the enzymes substrate – in the present case H_2 – is not near the saturation mixing ratio, which can be assumed in soils that do not show a significant production of H_2) it can be written as (compare e.g. Bisswanger, 1999)

$$\frac{dC_s}{dt} = -kC_s, \tag{4}$$

where k is a rate constant characteristic for the kinetic properties of the given enzyme (in this case *hydrogenases*). For our experiment, we have assumed no H_2 oxidation in the diffusive layer δ and that, at any point in time during the experiment, the hydrogen destruction in the catalytic centre equals the diffusive flux of substrate to the enzyme. This yields

$$\frac{dC_s}{dt} = \frac{dC_e}{dt} \tag{5}$$

so that, when combining (3) and (4), we get

$$\frac{P_{H_2}A}{\delta V}(C_e - C_s) = kC_s. \tag{6}$$

Solving (6) for C_s

$$C_s = \frac{C_e\frac{P_{H_2}A}{\delta V}}{k + \frac{P_{H_2}A}{\delta V}} \tag{7}$$

yields the effective substrate mixing ratio in the area around the reaction centre. Using (4) and (5), the actually determined H_2 destruction rate in the enclosure setup is given by

$$\frac{dC_e}{dt} = -k\frac{C_e\frac{P_{H_2}A}{\delta V}}{k + \frac{P_{H_2}A}{\delta V}} \tag{8}$$

or

$$\frac{dC_e}{dt} = -\frac{C_e}{\frac{1}{k} + \frac{\delta V}{P_{H_2}A}}. \tag{9}$$

For $k \ll \frac{P_{H_2}A}{\delta V}$ diffusive transport is much faster than the enzymatic reaction rate and (9) can be approximated by

$$\frac{dC_e}{dt} = -kC_e. \tag{10}$$

Contrary, for $k \gg \frac{P_{H_2}A}{\delta V}$ the enzymatic reaction becomes diffusion-controlled, that is,

$$\frac{dC_e}{dt} = -\frac{P_{H_2}A}{\delta V}C_e \tag{11}$$

and k has no measurable impact on the decline of H_2 inside the enclosure. Here, H_2 destruction is determined exclusively by diffusive properties of the medium in which the enzymatic reaction takes place. However, no matter if hydrogen destruction is controlled by the diffusive properties of the soil (11) or by the

kinetic properties of the enzyme (10), the temporal evolution of C_e inside the enclosure is described by a differential equation of the form

$$\frac{dC_e}{dt} = -\frac{1}{\tau}C_e \tag{12}$$

which is solved by an exponential function (compare inlay of Fig. 1)

$$C_e(t) = C_{e,o}e^{-\frac{t}{\tau}}. \tag{13}$$

Under field conditions we allowed for a possible production of H_2 inside the enclosure φ (ppb s^{-1}). So the mass balance (12) becomes

$$\frac{dC_e}{dt} = -\frac{1}{\tau}C_e + \varphi. \tag{14}$$

This is solved by

$$C_e(t) = (C_{e,o} - \varphi\tau)e^{-\frac{t}{\tau}} + \varphi\tau \tag{15}$$

which reduces to (13) for $\varphi = 0$ and returns the equilibrium mixing ratio $\varphi\tau$ for $t \to \infty$. In this study, the production φ was not further investigated.

In the two extreme cases (10) or (11) τ is given by

$$\tau = \begin{cases} 1/k, & \text{enzyme kinetics} \\ \frac{\delta V}{P_{H_2} A}, & \text{molecular diffusion.} \end{cases} \tag{16}$$

According to, for example, Bisswanger (1999), the kinetic constant k depends on temperature T, pH-value of the medium in which the enzymatic catalysis takes place and, of course, on the mixing ratio of enzymes C_{en} in the soil; the latter is possibly determined by the total organic carbon (TOC) content of the soil (Conrad and Seiler, 1985), thus

$$k = k(T, pH, C_{en}). \tag{17}$$

The effective diffusive permeability P of a gas in the soil air can be approximated with the Millington–Quirk Model (Millington and Quirk, 1959):

$$P_i = D_i \frac{(\Theta_p - \Theta_w)^{10/3}}{\Theta_p^2}, \tag{18}$$

where D_i is the molecular diffusion coefficient of the gas i in air, Θ_p is the total porosity of the soil and Θ_w is its volumetric moisture content. In the case of exclusive diffusion control of the uptake, the decay time τ of the hydrogen mixing ratio in the enclosure, can be written as

$$\tau = \frac{\delta V}{D_{H_2} A} \frac{\Theta_p^2}{(\Theta_p - \Theta_w)^{10/3}}. \tag{19}$$

It is dependent on the thickness of the flux restricting layer δ, the height ($h = V/A$) of the enclosure and on the physical properties of the soil. D_{H_2} is the molecular diffusion coefficient of hydrogen in air. τ can be transformed to a deposition velocity v_d via

$$v_d = \frac{h}{\tau} = \frac{P}{\delta}. \tag{20}$$

From v_d the uptake flux density j_{H_2} in g (m^2 s) can be calculated according to

$$j_{H_2} = -\frac{pC_{e,o}M_{H_2}}{RT} v_d. \tag{21}$$

Here, p is the atmospheric pressure, M_{H_2} is the molar mass of hydrogen, R is the universal gas constant and T is the temperature.

3. Methods

3.1. Sampling location

Regular enclosure measurements were done at the Grenzhof field site [49°24' N, 8°36' E], an agricultural area with loess loamy soil located about 10 km northwest of Heidelberg, Germany. In 2007 precipitation at the site was ≈ 590 mm, mean temperature ≈10.8 °C and the range of volumetric soil moisture at 13 cm was from 0.06 to 0.29. Six individual plots were sampled on a transect approximately 30 m apart. Sampling was performed at about monthly intervals over the period of August 2006 to December 2007. Here, we present only the results obtained from four plots on bare soil, since sampling over vegetated soil (partly clover) showed temporarily strong hydrogen production associated with nitrogen fixation (Conrad, 1996).

3.2. Sampling technique

Stainless steel frames, covering 0.25 m^2 of soil area were permanently installed on the plots. For enclosure measurements they were covered with a water-sealed Makrolon frame and top. Five air samples were collected from the enclosure at ambient pressure into 1 L glass flasks in time intervals of several minutes (see Fig. 1). Samples were analysed in the lab for H_2 mixing ratios (and SF_6 in the case of soil air, see 3.4) with the RGA-3 (Hewlett Packard) detector (electron capture detector for SF_6) of the Heidelberg Combi Gas Chromatographic System (Hammer, 2008). For routine air sample analysis at the Combi GC, a minimum amount of 170 ml (STP) gas sample per injection is needed where the sample loops are flushed for about 100 s with the overpressure in the sample flask at a flow rate of 100 ml min^{-1}. However, the samples to be analysed in this study have atmospheric pressure or – in the case of the soil samples – even less than ambient pressure. Therefore, the injection port of the Combi GC had to be connected upstream with a device for a pressurization of the flasks to achieve the necessary overpressure and flow through the GC sample loops. Pressurization of the flasks is performed with a standard gas of known H_2 (SF_6) mixing ratio C_{st} under defined conditions for pressure p and temperature T, so that the initial H_2 (SF_6) mixing ratio C_{in} in the flasks before the pressurization can be calculated from the measured mixing ratio and from a pressure measurement before and after the pressurization performed at a constant temperature T. The measured H_2 (SF_6)

Table 1. Porosity Θ_p, pH-value and TOC of the soil at the plot sites 1, 2, 4 and 5

Plot	1	2	4	5
Θ_p	0.40	0.40	0.38	0.36
pH-value	5.75	5.75	6.39	5.92
TOC (%)	0.55	0.55	0.73	0.72

Note: For sites 1 and 2 the same values are reported. Relative errors of Θ_p and pH-value range from 3% to 5% whereas the (absolute) error of TOC amounts to 1% of the absolute value.

mixing ratio C_{me} after the pressurization is given by

$$C_{me} = \frac{C_{in} p_1 + C_{st}(p_2 - p_1)}{p_2} \tag{22}$$

which follows from the linearity of the Ideal Gas Law. Here, p_1 and p_2 denote the pressure before and after the pressurization, respectively. This leads to

$$C_{in} = \frac{C_{me} p_2 - C_{st}(p_2 - p_1)}{p_1}, \tag{23}$$

the initial mixing ratio of the sample. The measurement precision for C_{in} was ± 5 ppb for H_2 and ± 3 ppt for SF_6.

3.3. Determination of additional soil parameters

Inside the enclosure air temperature T and pressure p were monitored throughout the whole sampling period. Integrated over the upper 10 cm, volumetric soil moisture content Θ_w was measured at each plot during each sampling event with time domain reflectometry (Robinson et al., 2003), calibrated according to Roth et al. (1990). For each plot the total porosity Θ_p, pH-value and TOC content were analysed by the Laboratory for Geomorphology and Geoecology of the University of Heidelberg (see Table 1).

3.4. SF_6 tracer experiment

The validity of the Millington–Quirk Model (eq. 18) to properly describe diffusive transport in the soil was tested with a tracer experiment. The air inside the enclosure was spiked with the inert gas SF_6 and the distribution of SF_6 in the soil air after the time t, $C_{SF_6}(z, t)$ was measured by collecting 50 ml samples from probes mounted in the soil below the enclosure. The SF_6 depth profile after time t can be described mathematically as a solution of Fick's second law

$$\frac{\partial C_{SF_6}}{\partial t} = P_{SF_6} \frac{\partial^2 C_{SF_6}}{\partial z^2}. \tag{24}$$

For the present case (24) is solved by (Crank, 1975)

$$C_{SF_6}(z, t) = C_{SF_6,0} \left(1 - \mathrm{erf}\left(\frac{z}{2\sqrt{P_{SF_6} t}}\right)\right), \tag{25}$$

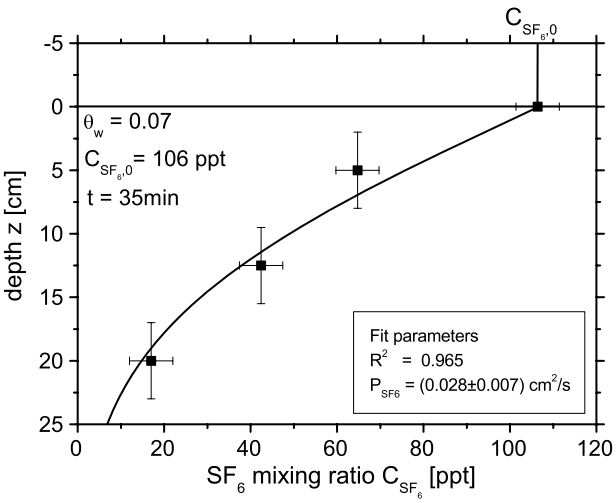

Fig. 2. Measured SF_6 depth profile after spiking with 106 ppt SF_6 and diffusion time t. The fit of eq. (25) to the data (solid curve) provides P_{SF_6}.

where $C_{SF_6,0}$ is the (approximately constant) SF_6 mixing ratio at the soil surface inside the enclosure and P_{SF_6} is the diffusive permeability of SF_6 in the soil. If the diffusion time t is known, P_{SF_6} can be obtained from a fit of (25) to the recorded depth profile (compare Fig. 2). At constant porosity Θ_p and soil moisture content Θ_w, P_i of a gas i is proportional to D_i (see eq. 18), that is,

$$P_i = B D_i. \tag{26}$$

The factor B is the same for every gas since it only depends on the properties of the soil. P_{H_2} can therefore be derived from P_{SF_6} via

$$P_{H_2} = \frac{D_{H_2}}{D_{SF_6}} P_{SF_6} \tag{27}$$

with $D_{SF_6} = 0.10\,\mathrm{cm^2\,s^{-1}}$ and $D_{H_2} = 0.63\,\mathrm{cm^2\,s^{-1}}$ (Lide and Frederikse, 1995).

4. Results

For each sampling event, the temporal evolution of the H_2 mixing ratio inside the enclosure was fitted using (15). The production rates φ resulting from the fits were sufficiently small to justify the assumption of zero production. Decay times τ varied from 8.4×10^2 to 8.9×10^3 s, which corresponds to a variation in deposition velocity v_d of 8.4×10^{-3} to $8.2 \times 10^{-2}\,\mathrm{cm\,s^{-1}}$ (compare eq. 20). At first we want to present the dependence of the obtained deposition velocities v_d on temperature T and soil moisture Θ_w(volumetric water content of the soil).

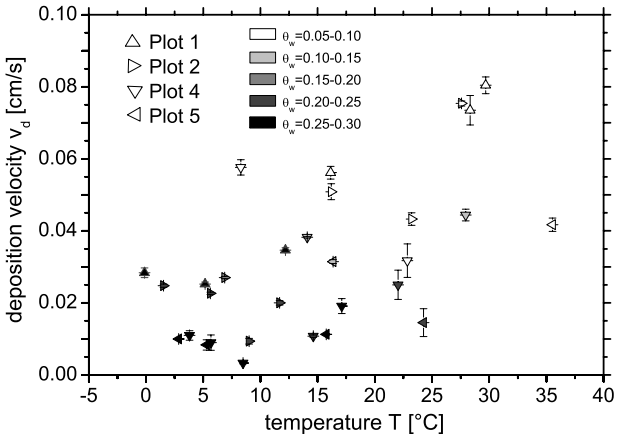

Fig. 3. Temperature dependence of the deposition velocity v_d for all plots. Darker shaded symbols indicate a higher moisture content of the soil (see legend).

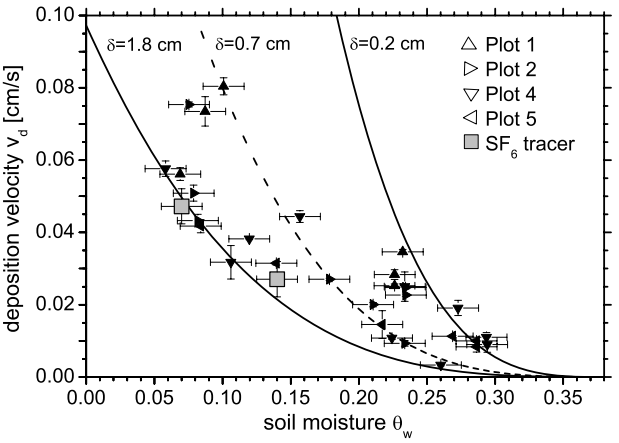

Fig. 4. Dependence of the deposition velocity v_d on soil moisture content. The mean total porosity Θ_p of the soil is 0.38. The solid curves are calculated functions according to eqs. (18) and (20) for two extremes of the flux restricting layer $\delta = 0.2, 1.8$ cm enclosing all measured data. The grey squares show the points obtained from the SF_6 tracer experiment for an assumed $\delta = 1.8$ cm.

4.1. Temperature dependence of v_d

Figure 3 shows the temperature (T) dependence of the deposition velocities v_d for the four different plots on bare soil and all sampling dates. The graph shows a tendentially higher deposition velocity at higher temperature. However, if one takes into account also the soil moisture level during sampling (grey shading of the data points), high deposition velocities are always associated with low soil moisture and vice versa. This suggests that the observed temperature dependence of the deposition velocity is overlayed by a soil moisture dependence and that the temperature dependence may be of secondary importance.

4.2. Soil moisture dependence of v_d

Figure 4 shows the relation between v_d and Θ_w for the four different plots and all sampling dates. It is clearly visible that v_d is strongly decreasing with rising Θ_w as was found earlier in other investigations (e.g. Conrad, 1996; Yonemura et al., 1999). It thus remains to quantify δ, the thickness of the flux restricting layer (Fig. 1) which can provide an estimate of the location of the enzymatic sink. If we assume exclusive diffusion control of the H_2 uptake over the whole moisture range eqs. (18) and (20) describe $v_d(\Theta_w)$ with the free parameter δ. With $D_{H_2} = 0.63\,\mathrm{cm^2\,s^{-1}}$ (Lide and Frederikse, 1995) for the molecular diffusion coefficient of H_2 in air at STP and $\Theta_p = 0.38$ for the mean total porosity of the soil on plots 1, 2, 4 and 5, all observed data fall into a range of $\delta = 0.2$ cm to $\delta = 1.8$ cm (Fig. 4). This confirms that the enzymatic reaction takes place within the uppermost few centimetres of the soil (Liebl and Seiler, 1976; Conrad, 1996; Yonemura et al., 2000a). The adequacy of the Millington–Quirk Model describing the moisture dependence of the permeability P_{H_2} (and therefore of v_d) for exclusive diffusion control of the uptake at the Grenzhof site studied here was validated with the SF_6 tracer experiment for two different soil moisture contents ($\Theta_w = 0.07, 0.14$) using eq. (16, lower case). One can see in Fig. 4 that the calculated data for v_d fit well the model curve for example, for $\delta = 1.8$ cm. This confirms that the Millington–Quirk Model is adequate to estimate $P_i(\Theta_w)$ for the investigated soil.

4.3. Dependence of v_d on additional soil parameters

Typical time constants τ of enzymatic reactions lie between 10^2 and 10^{-6} s (Voet et al., 2006), so all $\tau < 10^3$ s ($v_d > 0.027\,\mathrm{cm\,s^{-1}}$) can be potentially influenced by the kinetic properties of the enzyme as well. Since the time constant $1/k$ is as well dependent on temperature, pH-value and the TOC of the soil, a dependence of v_d on those parameters should be observable, at least for low moisture contents. In our case variations of pH and TOC in between the different sites were very small, so that these dependencies could not be studied. Although the temperature range was as large as 25 K, no significant dependence of v_d on temperature could be found, even for low soil moisture contents where the temperature dependence should possibly not be ruled out by an overlying moisture dependence. This could also be due to the data in this v_d-range being very scarce.

4.4. Model extrapolation

According to the observational findings presented above, soil uptake at our site is mainly influenced by soil moisture content. From Fig. 4 we see that the model assumption of exclusive diffusion control of the uptake fits well to the measured v_d and a range of δ between 0.2 and 1.8 cm. If we assume the model

Table 2. Range of observed H_2 deposition velocities v_d during different field studies with various soil types

Authors	Soil type	$v_d(10^{-2}\,\mathrm{cm\,s^{-1}})$	TOC (%)
Conrad and Seiler (1985)	Arid subtropical soil/Spain	0–3	0.5
Conrad and Seiler (1985)	Arid subtropical soil/South Africa (Karoo)	0–1	0.5
Conrad and Seiler (1985)	Arid subtropical soil/South Africa (Transvaal)	0–13	3.4
Yonemura et al. (1999)	Andisol field/Japan	0–10	-
Yonemura et al. (2000b)	Arable field/Japan	0–9	-
Yonemura et al. (2000b)	Forest soil/Japan	5–8	-
Lallo et al. (2008)	Forest soil/Finland	0–7	40-50
This study	Arable field/Germany	1–8	0.5-0.7

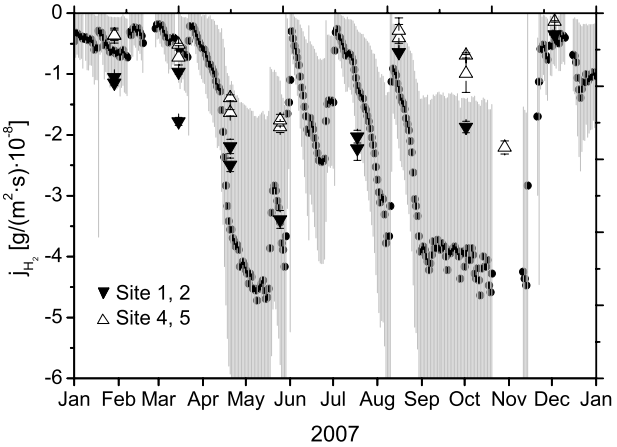

Fig. 5. Calculated deposition flux densities j_{H_2} according to eqs. (18), (20) and (21) derived from measured Θ_w, T, p, C_e and a mean $\delta =$ 0.7 cm in comparison to the measured flux densities (triangles).

to be valid, it should be possible to calculate daily and finally also annual means of the H_2 deposition flux j_{H_2} from eqs. (18), (20) and (21) if Θ_p, a mean δ as well as the meteorological parameters p, T, Θ_w and $C_{e,o}$ (which would then be the atmospheric H_2 mixing ratio) are known. This was done in Fig. 5 for the year 2007. A meteorological station close to plots 1 and 2 recorded atmospheric pressure p, temperature T and the soil moisture in 13 cm depth. (Since plots 4 and 5 are located in a small depression in the field, soil moisture values there were significantly higher at each sampling event. As the meteorological station only recorded moisture values near plots 1 and 2, only those plots were considered. For the atmospheric H_2 mixing ratio $C_{e,o}$ the continuous measurements observed in Heidelberg by Hammer (2008) were used. For the calculation of the fluxes, we took the daily means of the data. δ was taken from a fit of (20) (with τ according to eq. 19) to the data in Fig. 4, using only the results from plots 1 and 2, yielding a value of 0.7 cm. In Fig. 5, the black dots are the calculated daily means of j_{H_2} in [g/(m^{2}s)]. The error bars are calculated by gaussian error propagation of the standard deviations of the daily means in the used formula. The filled triangles are the measured data of field plots 1 and 2. These directly measured fluxes generally fit with the calculated values within their uncertainties which confirms the model assumptions. An annual mean H_2 uptake flux of $-2.0 \times 10^{-8}\,\mathrm{g/(m^2\,s)}$ was obtained from the model estimates. For comparison, we also plotted the measured data of field plots 4 and 5 in Fig. 5, indicated as open triangles. Directly measured fluxes on these plots are lower than those of plots 1 and 2, and yielded an annual mean value of $-1.7 \times 10^{-8}\,\mathrm{g/(m^2\,s)}$. This is another indication for the diffusion control of the uptake process, since plots 4 and 5 show a lower porosity (Table 1) and a higher water content throughout the year.

5. Discussion

Molecular hydrogen deposition velocities measured in the present study (i.e. 8.4×10^{-3} to $8.2 \times 10^{-2}\,\mathrm{cm\,s^{-1}}$) are well in the range of previously observed values (see Table 2). Comparison of individual data is difficult, since the studies were performed on different soil types and ecosystems. In particular, the different soil types may explain the variability of the observed maximum values for v_d, since the maximum H_2 destruction rate in a soil is probably dependent on its biochemical composition. From the field studies cited in Table 2, only Conrad and Seiler (1985) and Lallo et al. (2008) provide data on the TOC of the particular soil. However no correlation between TOC and the maximum uptake rate can be seen (Table 2).

As in the present work, the variability of v_d was also investigated with respect to its dependence on soil moisture content. Most studies find a strong dependence of H_2 uptake on soil moisture. Field studies (Table 2) as well as laboratory studies from Lallo et al. (2008), Smith-Downey et al. (2006) and Yonemura et al. (2000a) report a significant uptake inhibition for high soil moisture contents (water saturation >30–50%) and attribute this to the increasing diffusive resistance in the soil with increasing soil moisture content. In the present study, the variability of H_2 uptake could be attributed and quantitatively explained by the physical properties of the soil (Θ_p, Θ_w) assuming a flux restricting layer thickness δ between 0.2 and 1.8 cm. However, since

our study was performed on vegetation free soil, these results may not be valid if the soil structure is, for example, modified by plant roots. Furthermore, the model chosen to explain the diffusion control is quite simple. In real nature, this surface layer of the soil may be influenced by advective fluxes driven by pressure gradients or wind-pumping. Also, one might expect that in the uppermost flux restricting layer, which was assumed here to be inactive, also hydrogen breaking enzymes are present. However, at least a significantly lowered enzyme activity in that region of the soil may be justified by the laboratory work of Yonemura et al. (2000a).

We find a slight trend of increasing uptake towards higher temperatures (above 15 °C), however this trend can be attributed to the accompanying trend in soil moisture content. Moreover, in contrast to Smith-Downey et al. (2006) and Yonemura et al. (2000a), we do not find a defined temperature optimum. However, also Lallo et al. (2008) do not find a temperature dependence of v_d in the range of 2–27 °C. In fact, they report only a strong decrease of v_d for temperatures below 5 °C. This may, however, also be associated with wetter or even deeply frozen soil and thus largely reduced permeability during these situations.

6. Conclusions

The major finding of this field study performed on a vegetation free soil is that the variability of H_2 uptake can be largely explained by a transport restriction through a thin layer of thickness 0.2–1.8 cm at variable soil moisture content. Any existing temperature dependence is almost completely ruled out through this effect. Therefore, soil texture and moisture content appear to be reasonable properties to parametrize the soil sink of atmospheric H_2. The influence of microbiological properties of the soil (TOC etc.) as well as the pure temperature dependence at constant soil moisture, still need to be investigated.

We conclude that in a future hydrogen economy leading to an increasing atmospheric hydrogen mixing ratio both processes controlling the atmospheric H_2 sink strength, that is, diffusion of H_2 into the soil and enzymatic destruction, will increase. This effect may thus counteract the expected strong increase of the atmospheric H_2 burden.

7. Acknowledgments

The authors thank Ralf Conrad, Tobias Naegler and Felix Vogel for valuable discussions, Kurt Roth for making available the sampling site, providing equipment and for information on soil properties. Further we would like to thank Anna Wonneberger and Christian Ebert for their help in sample analysis and three anonymous reviewers for their helpful suggestions to improve this manuscript. This work was funded by the EuroHydros project of the European Union.

References

Bisswanger, H. 1999. *Enzyme Kinetics*. Wiley-VHC, Weinheim, Germany.

Conrad, R. 1996. Soil microorganisms as controllers of atmospheric trace gases (H_2, CO, CH_4, OCS, N_2O and NO). *Microbiol. Rev.* **60**, 609–640.

Conrad, R. and Seiler, W. 1981. Decomposition of atmospheric hydrogen by soil microorganisms and soil enzymes. *Soil Biol. Biochem.* **34**, 43–49.

Conrad, R. and Seiler, W. 1985. Influence of temperature, moisture, and organic carbon on the flux of H_2 and CO between soil and atmosphere: field studies in subtropical regions. *J. Geophys. Res.* **90**, 5699–5709.

Crank, J. 1975. *Mathematics of Diffusion*. Oxford University Press, London, UK.

Guo, R. and Conrad, R. 2008. Extraction and characterization of soil hydrogenases oxidizing atmospheric hydrogen. *Soil Biol. Biochem.* **40**, 1149–1154.

Hammer, S. 2008. *Quantification of regional H_2 sources and sinks derived from multi tracer analyses of continuous atmospheric measurements*. Ph.D. Thesis, University of Heidelberg.

Hauglustaine, D. A. and Ehhalt, D. H. 2002. A three dimensional model of molecular hydrogen in the troposphere. *J. Geophys. Res.* **107**, 4330.

Lallo, M. P., Aalto, T., Laurila, T. and Hatakka, J. 2008. Sesonal variations in hydrogen deposition to boreal forest soil in southern Finland. *Geophys. Res. Lett.* **35**, L04402.

Lide, D. and Frederikse, H. 1995. *CRC Handbook of Chemistry and Physics*. CRC Press, Boca Raton, FL.

Liebl, K. and Seiler, W. 1976. CO and H_2 destruction at the soil surface. In: *Microbial production and utilization of gases* (eds H. G. Schlegel et al.). E. Goltze, Göttingen, Germany, 215–229.

Millington, R. J. and Quirk, J. P. 1959. Permeability of porous media. *Nature* **183**, 387–388.

Novelli, P. C., Lang, P. M., Masarie, D. F., Myers, R. and co-authors. 1999. Molecular hydrogen in the troposphere: global distribution and budget. *J. Geophys. Res.* **104**, 427–444.

Rhee, T. S., Brenninkmeijer, C. and Röckmann, T. 2006. The overwhelming role of soils in the global atmospheric hydrogen cycle. *Atmos. Chem. Phys.* **6**, 1611–1625.

Robinson, D. A., Jones, S. B., Wraith, J. M., Or, D. and Friedman, S. P. 2003. A review of advances in dielectric and electrical conductivity measurement in soils using time-domain reflectometry. *Vadose Zone J.* **2**, 444–475.

Roth, K. R., Schulin, R., Flühler, H. and Attinger, W. 1990. Calibration of time domain reflectometry for water content measurement using a composite dielectric approach. *Water Resour. Res.* **67**, 2267–2273.

Schultz, M. G., Diehl, T., Brasseur, G. P. and Zittel, W. 2003. Air pollution and climate-forcing impacts of a global hydrogen economy. *Science* **302**, 624–627.

Smith-Downey, N., Randerson, T. and Eiler, J. M. 2006. Temperature and moisture dependence of soil H_2 uptake measured in the laboratory. *J. Geophys. Res.* **33**, L14813.

Tromp, T. K., Shia, R. L., Allen, M. and Eiler, J. M. 2003. Potential environmental impact of a hydrogen economy on the stratosphere. *Science* **300**, 1740–1742.

Voet, D., Voet, J. and Pratt, C. 2006. *Fundamentals of Biochemistry*. John Wiley and Sons, New York, NY.

Yonemura, S., Yokozawa, M., Kawashima, S. and Tsuruta, H. 1999. Continuous measurements of CO and H_2 deposition velocities onto an andisol: uptake control by soil moisture. *Tellus* **51B**, 688–700.

Yonemura, S., Yokozawa, M., Kawashima, S. and Tsuruta, H. 2000a. Model analysis of the influence of gas diffusivity in soil and on CO and H_2 uptake. *Tellus* **52B**, 919–933.

Yonemura, S., Kawashima, S. and Tsuruta, H. 2000b. Carbon monoxide, hydrogen, and methane uptake by soils in a temperate arable field and a forest. *J. Geophys. Res.* **105**, 347–362.